Technical Notes

TECHNICAL NOTES are short manuscripts describing new developments or important results of a preliminary nature. These Notes cannot exceed 6 manuscript pages and 3 figures; a page of text may be substituted for a figure and vice versa. After informal review by the editors, they may be published within a few months of the date of receipt. Style requirements are the same as for regular contributions (see inside back cover).

Transpiration Cooling in Three-Dimensional Laminar Boundary-Layer Flow near a Stagnation Point

D. R. JENG*
University of Toledo, Toledo, Ohio
AND
DONALD W. WILLIAMS†
University of Alabama, Huntsville, Ala.

ONE effective method of reducing the heat-transfer coefficient is so called transpiration cooling; for example, by the use of porous surfaces through which a coolant is injected. Hartnett and Eckert[1] have studied the transpiration cooling in a laminar boundary layer for the flow over the flat plate and two-dimensional stagnation flow. Later, this problem was extended by Sparrow et al.[2] for an electrically conducting fluid with the action of magnetic field in two-dimensional and axisymmetrical stagnation flows. The purpose of this Note is to investigate the transpiration cooling at the general three-dimensional stagnation point in laminar boundary layer. The study is concerned with the prediction of the skin friction, heat transfer, and required coolant flows for such transpiration cooled surfaces.

Following the arguments given by Howarth[3,4] in his study of three-dimensional boundary-layer flow, the coordinate system near the stagnation point of regular surface may be described by the Cartesian system (x, y, z) as shown in Fig. 1.

For the steady laminar flow with negligible dissipation of an incompressible fluid with constant properties, the governing boundary-layer equations for the title problem are

$$\frac{\partial u}{\partial x}+\frac{\partial v}{\partial y}+\frac{\partial w}{\partial z}=0 \tag{1}$$

$$u\frac{\partial u}{\partial x}+v\frac{\partial u}{\partial y}+w\frac{\partial u}{\partial z}=-\frac{1}{\rho}\frac{\partial p}{\partial x}+\nu\frac{\partial^2 u}{\partial y^2} \tag{2a}$$

$$u\frac{\partial w}{\partial x}+v\frac{\partial w}{\partial y}+w\frac{\partial w}{\partial z}=-\frac{1}{\rho}\frac{\partial p}{\partial z}+\nu\frac{\partial^2 w}{\partial y^2} \tag{2b}$$

$$u\frac{\partial T}{\partial x}+v\frac{\partial T}{\partial y}+w\frac{\partial T}{\partial z}=\alpha\frac{\partial^2 T}{\partial y^2} \tag{3}$$

with velocity boundary conditions

$$u(x,0,z)=w(x,0,z)=0 \tag{4}$$

$$v(x,0,z)=v_w \tag{5}$$

$$u(x,\infty,0)=K_x x \tag{6}$$

$$w(0,\infty,z)=K_z z \tag{7}$$

Where v_w is the normal velocity of the fluid at the wall. Positive values denote injection and negative values denote suction. The constants K_x and K_z represent the velocity gradients outside the boundary layer, respectively, in x and z directions. The boundary conditions for the temperature field are

$$T(x,0,z)=T_w \tag{8}$$

$$T(x,\infty,z)=T_\infty \tag{9}$$

Introducing the Howarth similarity transformation[4] defined by

$$u=K_x x f'(\eta) \tag{10a}$$

$$w=K_z z g'(\eta) \tag{10b}$$

$$v=-(\nu/K_x)^{1/2}[K_x f(\eta)+K_z g(\eta)] \tag{10c}$$

$$\eta=y(K_x/\nu)^{1/2} \tag{11}$$

and the dimensionless temperature

$$\theta=(T-T_\infty)/(T_w-T_\infty) \tag{12}$$

into Eqs. (2–7), then the momentum and energy equations become

$$f'''+(f+Cg)f''=(f')^2-1 \tag{13a}$$

$$g'''+(f+Cg)g''=C[(g')^2-1] \tag{13b}$$

$$\theta''+Pr(f+Cg)\theta'=0 \tag{14}$$

with boundary conditions

$$f(0)=g(0)=-\frac{v_w}{(1+c)(\nu K_x)^{1/2}}=A_0 \tag{15}$$

$$f'(0)=g'(0) \tag{16}$$

$$\theta(0)=1 \tag{17}$$

$$f'(\infty)=g'(\infty)=1 \tag{18}$$

$$\theta(\infty)=0 \tag{19}$$

The primes designate derivatives with respect to η while f, g, and θ are functions of η only.

The parameter $C=K_z/K_x$ represents the ratio of the velocity gradients in two principal directions x and z, just outside the boundary layer. Obviously, the case $C=0$ corresponds to the two-dimensional stagnation flow while $C=1$ corresponds to the axisymmetrical stagnation. If the x coordinate is identified with the major principal curvature, then all stagnation flow would have $0 \leq C \leq 1$. Another parameter $A_0=f(0)=g(0)$ is referred to as a mass transfer parameter. Since the present problem concerns the transpiration cooling, only the negative value will be considered in the present analysis. The continuity equation (1) will not be involved in the calculation, because of that with (10), this equation is automatically satisfied.

The numerical solutions of (12) and (13) with the appropriate boundary conditions have been obtained using Univac 1107 computer by the Runge-Kutta iterative method. The results for $f''(0)$ and $g''(0)$ are tabulated in Table 1 for the range of C and A_0 shown. To determine the range of A_0, the following fact should be noted. The blowing velocity v_w should be sufficiently small that the boundary-layer character is preserved. The values of $-A_0$ were assigned from 0 to 2 for C ranging from 0 to 0.5

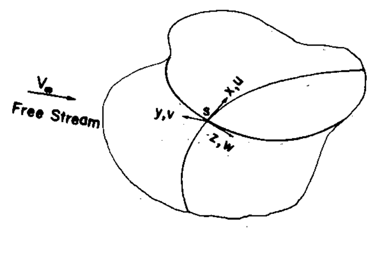

Fig. 1 Coordinate system for general three-dimensional stagnation point.

Received February 16, 1973.
Index categories: LVIM Aerodynamic Heating; Boundary Layers and Convective Heat Transfer—Laminar.

* Associate Professor of Mechanical Engineering.

† Graduate Student—Division of Engineering.

Table 1 Values of $f''(0)$ and $g''(0)$

C		$-A_0$ 0	0.5	1.0	1.5	2.0
0	$f''(0)$	1.2326	0.9692	0.7566		0.4758
	$g''(0)$	0.5705	0.2950	0.1168		0.005618
0.25	$f''(0)$	1.2476	0.9205	0.6736		0.3914
	$g''(0)$	0.8051	0.4700	0.2548		0.1032
0.5	$f''(0)$	1.2669	0.8777	0.6035		0.3304
	$g''(0)$	0.9981	0.6047	0.3553		0.1684
0.75	$f''(0)$	1.2887	0.8390	0.5435	0.3373	
	$g''(0)$	1.1643	0.7131	0.4317	0.2882	
1.0	$f''(0)$	1.3119	0.8036	0.4919	0.3332	
	$g''(0)$	1.3119	0.8036	0.4919	0.3332	

and 0 to 1.5 for C took the values larger than 0.5, since for a fixed value of $-A_0$ the blowing velocity increases as C increases. The numerical data for $f''(0)$ and $g''(0)$ given in Table 1 may be used for evaluating skin friction. Furthermore, these informations will be used later in heat-transfer calculation. The data for two-dimensional and axisymmetrical cases with $A_0 = 0$ are recalculated by us and also included in the table for the sake of the comparison of the accuracy with available date.[4] Present data closely agree with those of Howarth[4] but the present calculations are carried to the accuracy of four decimal places instead of three. From the table, it may perhaps be remarked that changes with C and A_0 are seen to be relatively small for the velocity component in the x direction, but quite marked in z-direction. The skin-friction components at the surface are given by

$$\begin{aligned} \tau_{yx} &= \rho v^{1/2} K_x^{3/2} x f''(0) \\ \tau_{yz} &= \rho v^{1/2} K_x^{3/2} C z g''(0) \end{aligned} \tag{20}$$

It can also be seen that increase of $-A_0$ will reduce the wall shear stress especially in z-direction.

With the momentum equation solved, a solution for the energy equation (14) can be obtained. The results for $\theta'(0)$ are tabulated in Table 2 for the range of C, A_0 and Prandtl number as shown. These values may be used in evaluating the heat transfer at the stagnation point. The data obtained in the present calculations closely agree with those given by Sparrow et al.[2] for two-dimensional and axisymmetrical cases except for Prandtl number of 10. Some of the values for this Prandtl number differ considerably. An extensive presentation of temperature profiles will not be given here. However, Fig. 2 shows a small sampling of profiles. It is noted that for the same mass transfer parameter A_0, C has little effect but Prandtl number has significant effect on the shape of the temperature profiles. The results for $Pr = 0.01$ should be used with reservation. Under

Table 2 Values of $-\theta'(0)$

	C 0	0.25	0.5	0.75	1.0
$-A_0$			$Pr = 0.01$		
0	0.07597	0.08432	0.09212	0.09940	0.1062
0.5	0.07217	0.07920	0.08577	0.09191	0.09763
1.0	0.06830	0.07384	0.07906	0.08392	0.08845
1.5				0.07580	0.07925
2.0	0.06051	0.06300	0.06553		
			$Pr = 0.1$		
0	0.2195	0.2408	0.2619	0.2822	0.3015
0.5	0.1850	0.1958	0.2069	0.2177	0.2278
1.0	0.1525	0.1530	0.1551	0.1574	0.1596
1.5				0.1058	0.1028
2.0	0.09540	0.8178	0.07260		
			$Pr = 0.7$		
0	0.4959	0.5362	0.5797	0.6231	0.6654
0.5	0.2933	0.2824	0.2777	0.2750	0.2728
1.0	0.1457	0.1123	0.9073×10^{-1}	0.7523×10^{-1}	0.6328×10^{-1}
1.5				0.1021×10^{-1}	0.6385×10^{-2}
2.0	0.1687×10^{-1}	0.500×10^{-2}	0.1671×10^{-2}		
			$Pr = 1.0$		
0	0.5704	0.6153	0.6644	0.7139	0.7622
0.5	0.2950	0.2740	0.2615	0.2523	0.2444
1.0	0.1168	0.7952×10^{-1}	0.5742×10^{-1}	0.4295×10^{-1}	0.3280×10^{-1}
1.5				0.2515×10^{-2}	0.1250×10^{-2}
2.0	0.5617×10^{-2}	0.9502×10^{-3}	0.1912×10^{-3}		
			$Pr = 10$		
0	1.3389	1.4263	1.5314	1.6417	1.7521
0.5	0.2703×10^{-1}	0.8833×10^{-2}	0.3340×10^{-2}	0.2010×10^{-2}	0.6270×10^{-3}
1.0	0.7419×10^{-5}	0.9149×10^{-7}	0.1776×10^{-8}	0.4997×10^{-10}	0.1828×10^{-11}
1.5				0.1927×10^{-22}	0.9187×10^{-26}
2.0	0.5241×10^{-18}	0.4258×10^{-26}	0.2020×10^{-33}		

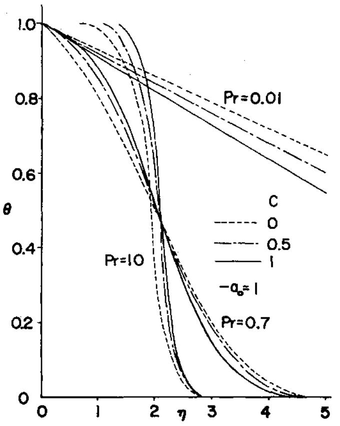

Fig. 2 Dimensionless temperature profiles for $A_0 = -1$.

this condition, the thermal boundary-layer thickness is much greater than that of the velocity boundary layer and the usual boundary-layer approximation implicit in Eq. (3) may become poor.

The heat flux at the surface is given by

$$q_w = -k \left.\frac{\partial T}{\partial y}\right|_{y=0} = -k(T_w - T_\infty)\left(\frac{K_x}{v}\right)^{1/2} \theta'(0) \tag{21}$$

Introducing the Nusselt number

$$Nu = \frac{q_w(xU_\infty/K_x)^{1/2}}{k(T_w - T_\infty)}$$

and the Reynolds number $Re = xU_\infty/v$, Eq. (21) may be rewritten as

$$Nu/Re^{1/2} = -\theta'(0) \tag{22}$$

The value of $Nu/Re^{1/2}$ increases with increasing C for fixed value of $-A_0$ and Prandtl number. The transpiration cooling becomes the more effective, the larger the Prandtl number becomes and for fixed value of C, the effectiveness of the blowing in reducing the heat transfer will become more prevalent when the Prandtl number increases.

References

[1] Hartnett, J. P. and Eckert, E. R. G., "Mass-Transfer Cooling in a Laminar Boundary Layer With Constant Fluid Properties," *Transactions of the ASME*, Vol. 79, 1957, pp. 247–254.

[2] Sparrow, E. M., Eckert, E. R. G., and Minkowyez, W. J., "Transpiration Cooling in a Magnetohydrodynamic Stagnation Point Flow," *Applied Scientific Research*, Sec. A, Vol. 11, 1962, pp. 125–147.

[3] Howarth, L., "The Boundary Layer in Three Dimensional Flow," Pt. I, "Derivation of the Equations for Flow Along a General Surface," *Philosophical Magazine*, Vol. 7s, No. 42, 1951, pp. 239–244.

[4] Howarth, L., "The Boundary Layer in Three Dimensional Flow," Pt. II, "The Flow Near a Stagnation Point," *Philosophical Magazine*, Vol. 7s, No. 42, 1951, pp. 1433–1440.

Droplet Dynamics in a Hypersonic Shock Layer

N. A. Jaffe*

Acurex Corp./Aerotherm Division, Mountain View, Calif.

Introduction

Hypersonic vehicles may encounter condensed water vapor in the form of either ice particles or liquid droplets. Particle deceleration and ablation effects in the shock layer were considered by Waldman and Reinecke.[1] These effects are coupled; however, in Ref. 1 velocities employed in the energy equation were taken from a constant mass solution to the momentum equation. In addition, the heat transfer in Ref. 1 was scaled with the particle velocity cubed (U^3). One stated objective was to obtain closed form solutions; however, only numerical solutions were obtainable for the energy equation. If the equations are treated in a coupled manner, closed form solutions are obtainable for both momentum and energy equations. It is felt that scaling the heat transfer as U^3 leads to even more serious errors than neglect of coupling. This scaling was adopted in order to relate the over-all heat-transfer rate, to the particle, to its stagnation value. This treatment is valid for a body in a cold freestream; in the limit it yields the result that there is no heat transfer to a cold particle stationary in the shock layer, relative to the vehicle. References 2–4 indicate that particle heating rates can be expressed in terms of a mean temperature drop ΔT_m, and Nusselt number Nu_m over a wide range of conditions for subsonic and supersonic flow and a much weaker dependence on velocity than is employed in the model used in Ref. 1. Indeed the Nusselt number variation is small over a Reynolds number range of several orders of magnitude.[4] Thus, in the present analysis the heat transfer is modeled with a Nusselt number and the equations remain coupled.

Received February 26, 1973; revision received June 18, 1973.

Index category: Fluid Dynamics, Thermophysics and Thermochemistry.

* Staff Engineer.

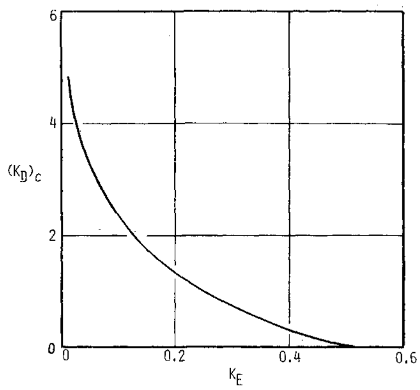

Fig. 1 Critical ablation curve.

Analysis

The energy equation for a particle of mass m, can be written

$$Q^*(dm/dt) = -\dot{Q} \tag{1}$$

The quantities $\dot{Q}$ and Q^* are the net heat rate (average heat flux x area) to the particle and the particle effective heat of ablation. The momentum equation along the stagnation streamline is

$$m(dU/dt) = -\tfrac{1}{2}C_D A\rho_s U^2 \tag{2}$$

where C_D is the particle drag coefficient based on cross-sectional area A; σ and ρ_s are particle and shock layer densities. The preceding equations are written in a coordinate system fixed with respect to the vehicle. It is assumed that the gas velocity in the shock layer is negligible compared to the particle velocity. If mass loss is assumed to take place as a result of fusion then Q^* must include the latent heat of fusion; if vaporization is the mechanism for mass loss then the heat of vaporization must also be included. Equation (1) implies that potential rate controlling processes such as phase change kinetics and diffusion have been neglected; thus, the results of the analysis represent a bounding case for mass transfer effects.

The equations are subsequently written for a spherical particle of radius r. The quantity $\dot{Q}$ is written in terms of a mean heat-transfer coefficient h_m and temperature drop ΔT_m

$$\dot{Q} = 4\pi r^2 h_m \Delta T_m \tag{3}$$

where